

Published in final edited form as:

Nat Cell Biol. 2014 June ; 16(6): 516–528. doi:10.1038/ncb2965.

The ability of inner cell mass cells to self-renew as embryonic stem cells is acquired upon epiblast specification

Thorsten Boroviak¹, Remco Loos², Paul Bertone^{1,2,3}, Austin Smith^{1,5}, and Jennifer Nichols^{1,4,*}

¹Wellcome Trust – Medical Research Council Cambridge Stem Cell Institute, University of Cambridge, Tennis Court Road, Cambridge CB2 1QR, UK, thorsten.boroviak@cscr.cam.ac.uk

²European Molecular Biology Laboratory, European Bioinformatics Institute, Wellcome Trust Genome Campus, Cambridge CB10 1SD, UK, remco@ebi.ac.uk

³Genome Biology and Developmental Biology Units, European Molecular Biology Laboratory, Meyerhofstraße 1, 69117 Heidelberg, Germany, bertone@ebi.ac.uk

⁴Department of Physiology, Development and Neuroscience, University of Cambridge, UK, austin.smith@cscr.cam.ac.uk

⁵Department of Biochemistry, University of Cambridge, UK

Abstract

The precise relationship of embryonic stem cells (ESC) to cells in the mouse embryo remains controversial. We present transcriptional and functional data to identify the embryonic counterpart of ESC. Marker profiling shows that ESC are distinct from early inner cell mass (ICM) and closely resemble preimplantation epiblast. A characteristic feature of mouse ESC is propagation without ERK signalling. Single-cell culture reveals that cell autonomous capacity to thrive when the ERK pathway is inhibited arises late during blastocyst development and is lost after implantation. The frequency of deriving clonal ESC lines suggests that all E4.5 epiblast cells can become ESC. We further show that ICM cells from early blastocysts can progress to ERK-independence if provided with a specific laminin substrate. These findings suggest that formation of the epiblast coincides with competence for ERK-independent self-renewal *in vitro* and consequent propagation as ESC lines.

Introduction

Mammalian preimplantation development establishes the founding cell population of the foetus and specifies two extraembryonic lineages. In mouse, at around the 16-cell stage, the outer cells acquire trophoblast identity; the interior cells form inner cell mass (ICM), which subsequently segregates into primitive endoderm (PrE) and preimplantation epiblast. Epiblast cells express pluripotency factors such as Oct4, Sox2 and Nanog1–5, whereas PrE

Users may view, print, copy, and download text and data-mine the content in such documents, for the purposes of academic research, subject always to the full Conditions of use:http://www.nature.com/authors/editorial_policies/license.html#terms

*Corresponding Author, jn270@cam.ac.uk.

identity is established by sequential activation of *Gata6*, *Pdgfra*, *Sox17*, *Gata4* and *Sox76–11*.

Embryonic stem cells (ESC) are derived from murine ICMs. ESC retain full developmental potential when cultured on mitotically-inactivated fibroblast feeders^{12, 13} or in serum and leukaemia inhibitory factor (LIF)^{14, 15}. The unrestricted potential to produce all lineages, including the germline, has been termed ‘naïve’ pluripotency^{16, 17}. ESC differentiation is suppressed by inhibition of the mitogen-activated protein kinase (MAPK) signalling cascade^{18, 19}. A defined ESC culture regime, termed 2i, utilises the Mek inhibitor PD0325901 (PD03) to block the Erk pathway, and glycogen synthase kinase 3 inhibition by CHIR99021 (CHIR)²⁰. Addition of LIF is beneficial, but not required²¹. ‘Primed’ pluripotent cells derived from postimplantation epiblast (EpiSC)^{22, 23} have different signalling properties, requiring Activin and FGF for self-renewal. EpiSC generally die in 2i-LIF²⁴, suggesting that the ability to thrive in this medium is a distinctive feature of mouse ESC. Naïve pluripotent cells can be selected using 2i-LIF during reprogramming^{25, 26} and for derivation of germline competent ESC from previously non-permissive mouse strains and rats^{27–30}.

Although ESC are commonly derived from the ICM, they can be propagated from any preimplantation stage^{31, 32}. Even single blastomeres can become ESC, when aggregated with an existing colony³³ or on feeders with adrenocorticotrophic hormone³⁴. Furthermore, postimplantation epiblasts can be ‘epigenetically reprogrammed’ to ESC by extended culture in serum-LIF³⁵, questioning whether ESC relate to a native embryonic state. ESC were recently suggested to cycle through a rare, transient cell population with some similarities to the 2-cell stage³⁶. Hence, the exact origin of ESC and their relationship to embryonic cells *in vivo* remains controversial.

We identify the closest counterpart of ESC in the early embryo by comparative profiling and functional analysis of early embryonic cells at a single-cell level. We show that the ability of ICM cells to self-renew as ESC is acquired upon epiblast specification, defining this tissue as the *in vivo* origin of naïve pluripotency and providing a paradigm for seeking an equivalent state in embryos of other mammals.

Results

Transcriptional profiling of defined lineages in pre- and postimplantation mouse embryos

We established a gene expression profiling system to compare embryonic samples and cultured ESC directly. Preimplantation embryos contain only picogram amounts of RNA; therefore we utilised single-cell whole transcriptome amplification techniques^{37, 38}. Using groups of 10–20 cells allowed detection of changes in low-level gene expression, such as upregulation of *Socs3* in response to LIF-stimulation (Supplementary Fig.1A). We assessed 35 well-characterised lineage markers and 61 pathway-associated genes by quantitative real-time reverse-transcription PCR (qRT-PCR) (Fig.1a). The sensitivity of the experimental setup was tested with conventional and pre-diluted, subsequently preamplified cDNAs from bulk culture ESC (Supplementary Fig.1B). We examined individual embryos at various developmental stages from embryonic day (E)1.5 (2-cell) to postimplantation (E5.5) (Fig.

1b). Early cleavage embryos (E1.5 and E2.5) were assayed whole, whereas from later stages (E3.5, E4.0 and E4.5), ICMs were isolated by immunosurgery³⁹. To distinguish epiblast from PrE, embryos from platelet-derived growth factor receptor alpha H2B-GFP (*Pdgfra::GFP*) reporter mice^{40, 41} were used.

To validate the assay, we analysed the expression of known lineage markers. Genes characteristic of the morula stage, such as *Dppa3* (Stella) and *Pou5f1* (encoding Oct4) were robustly expressed at E2.5 (Fig.1c). E3.5 and E4.0 ICMs exhibited expression of *Nanog*, *Sox2*, *Klf2*, *Klf4*, *Bmp4* and *Fgf4* (Fig.1c,d), consistent with previous single-cell expression studies^{3, 4, 38}. The PrE markers *Gata6*, *Sox17*, *Gata4*, and *Pdgfra* were upregulated in *Pdgfra::GFP*-positive cells (Fig.1c). Cells negative for GFP did not express these markers, but exhibited substantially higher levels of *Klf2*, *Zfp42* (Rex1), *Utf1*, *Bmp4* and *Tdgf1* and moderately higher levels of *Pou5f1*, *Gdf3*, *Tfcp2l1* and *Nr0b1* (Dax1) (Fig.1c,d). Our dataset faithfully recapitulates the high expression of *Nanog* in early and mid-blastocyst stage ICMs and subsequent downregulation just before implantation, as previously published². *Klf4* was expressed in both epiblast and PrE, while *Klf2* was exclusive to epiblast. This confirms previous findings in which single-cell samples were annotated according to transcriptional profile⁴. We conclude that our data, based on 10-20 cells per lineage, accurately reflects patterns of gene expression previously observed in the developing mouse embryo^{3, 4, 38}.

Analysis of the postimplantation epiblast provides an opportunity to compare pluripotent states *in vivo*. At E5.5 *Fgf5*, *Nodal* and *Lef1* were upregulated, but no expression of *T*, *Cer1* and *Foxa2* was detected. Significantly, we found that ESC-specific naïve pluripotency markers^{17, 23, 24}, such as *Tbx3*, *Klf2*, *Klf4*, *Klf5*, *Dppa3*, *Fbxo15*, *Zfp42* and *Tfcp2l1* (Fig. 1c) were specific to preimplantation development. To provide insight into signalling processes operative in the early embryo, two thirds of the genes tested were associated with signalling pathways. We focused on a subset of key ligands, receptors and downstream targets of seven major signalling pathways (Fig.1d, Supplementary Fig.1c). *Socs3*, a direct target and negative regulator of Jak-Stat signalling^{42, 43} peaked at the 8-cell stage and was subsequently downregulated. In the early blastocyst ICM *Bmp4* was strongly upregulated, consistent with previous observations^{4, 44}. *Bmp4* expression was highest in the E4.5 epiblast and subsequently decreased. Strong expression of downstream targets *Id1* and *Id3* suggested that Bmp signalling was active in the epiblast. From E4.5 onwards, Activin-Nodal signalling-associated genes, such as *Nodal*, *Acvr2b* and their direct targets *Lefty1*, *Lefty2*⁴⁵ were upregulated (Fig.1d). FGF-MAPK signalling-associated genes were dynamically expressed throughout the stages analysed, while *Dkk1*, an inhibitor of Wnt signalling, was specifically upregulated in the E4.5 PrE (Fig.1d).

To visualise the relationship between populations we performed principal component analysis (PCA) (Fig.1e) and hierarchical clustering (Supplementary Fig.1D). The data largely clustered according to the developmental stage. Occasionally, samples resembled those of the next assigned embryonic stage, reflecting developmental variability between embryos.

These results demonstrate specific expression of naïve pluripotency markers in pre-, but not postimplantation embryos and suggest distinct waves of signalling pathway activities during early mouse development.

ESC are most similar to the preimplantation epiblast

To relate cultured ESC to embryonic lineages, we established ESC expression profiles using the same methodology. In contrast to previous studies³⁸ we used serum-free 2i culture²⁰. ESC in 2i exhibit lower expression of lineage-associated genes and more homogeneous expression of naïve pluripotency markers^{20, 46, 47}. Initially, we analysed groups of 10, 20 and 30 manually picked ESC in duplicate and compared the gene expression of ESC (E14TG2a) cultured in 2i versus 2i-LIF on gelatin. Unsupervised hierarchical clustering clearly separated cells cultured in the two conditions regardless of the amount of starting material (Fig.2a). Groups of 20 cells were used for all subsequent samples of cultured cells. We analysed a second ESC line (Rex1-GFP) derived from strain 129 and a further two lines (FL4, FL11) from F1 (CBAxC57BL/6) in 2i and 2i-LIF. PCA revealed that the majority of ESC samples cultured in 2i cluster with greatest similarity to the preimplantation epiblast (Fig.2b), a trend that increased in the presence of LIF. Hierarchical clustering grouped all ESC in 2i and 2i-LIF closest to E4.5 epiblast (Fig.2c, Supplementary Fig.2).

We also compared the expression of ESC cultured in conventional conditions. Rex1-GFP (RG) ESC were maintained for three passages in serum-LIF on gelatin and four samples of 20 randomly-chosen cells processed for transcriptional analysis. PCA showed that ESC in serum-LIF were widely scattered (Fig.2d), consistent with their reported heterogeneity^{46, 47}. Additionally, we analysed RG cells cultured in serum-LIF on feeders. The Rex1-positive cells and one of the four serum-LIF samples on gelatin clustered together close to the E4.5 epiblast, similar to ESC in 2i and 2i-LIF (Fig.2d,e). However, the Rex1-negative population and three of the four serum-LIF samples on gelatin fell between E5.5 epiblast and extraembryonic visceral endoderm, suggesting partial differentiation and exit from naïve pluripotency (Fig.2d,e). To investigate how this correlates with later ('primed') states of pluripotency, we included two independent EpiSC samples. Both clustered tightly with the postimplantation epiblast (Fig.2e). In two-dimensional PCA, EpiSC located distinct from, but in proximity to, two RG serum-LIF samples, Rex1-negative ESC and E5.5 epiblast (Fig. 2d). Thus, we can distinguish distinct pluripotent states by marker expression profiling and correlate those to specific embryonic lineages.

Independence from ERK-signalling emerges at the mid-blastocyst stage and is lost during implantation

Our transcriptional data highlight the similarity between naïve pluripotent ESC and the preimplantation epiblast. These cell types may also share functional characteristics. A distinctive feature of naïve ESC is their capacity for clonal propagation in 2i-LIF^{20, 24}. We confirmed that ESC can be efficiently derived in 2i-LIF from various preimplantation stages (Supplementary Fig.3a,b). The embryonic stage did not alter the characteristics of the resulting ESC, as previously demonstrated^{31, 32}. This suggests that embryonic cells within whole-embryo explants progress to a common stage in development from which they can be propagated as ESC. Consistent with this, we observed blastocyst formation (Supplementary

Fig.3C) and PrE-like epithelial structures during derivation from morulae (Supplementary Fig.3D).

To determine the developmental stage(s) at which embryonic cells can undergo autonomous self-renewal, we performed ESC derivation from dissociated cells using the stringent 2i-based culture regime as an assay (Fig.3a). Single-cells from 8-cell stage to postimplantation egg cylinder were manually transferred into individual culture wells to prevent intercellular signalling. The number of primary ESC colonies was assessed at day 7. We employed mating crosses from *Pdgfra::GFP* males with F1 females. Immunosurgically isolated E4.5 ICMs exhibited specific labelling of PrE (Fig.3b), resulting in clearly separable GFP-positive and negative cells (Fig.3c). We tested this defined ESC derivation system at the mid-blastocyst stage (E4.0) in 2i-LIF. Single-cells were deposited into individual wells (Fig.3d), resulting in primary ESC colonies (Fig.3e) which could readily be expanded to clonal ESC lines (Fig.3f). Blastocyst injection resulted in high contribution chimeras with germline transmission, confirming their functional equivalence to whole ICM-derived ESC (Fig.3g).

We first characterised derivation efficiencies of epiblast cells in 2i on gelatin. Single-cell ESC derivation efficiency is defined here as the percentage of wells per embryo that generated ESC colonies. ICMs from mid-late blastocyst stages (E3.75-E4.5) were more resistant to dissociation than earlier stages (E2.5-E3.5). Therefore cells from later preimplantation stages sometimes remained as duplets or triplets (Fig.3h,i, striped bars). We obtained a few ESC colonies from E3.75-E4.5 (Fig.3h). However, addition of LIF increased derivation efficiency to an average of 11% (ESC-containing wells per embryo) at E3.75-E4.0, increasing to 16% at E4.25-E4.5 (Fig.3i). Over 50% of these colonies were derived from single-cells (Fig.3i, non-striped bars). Single-cells from morulae and early blastocysts cultured in 2i-LIF (Fig.3j), but not 2i alone (Supplementary Fig.3E), persisted in culture for prolonged periods, occasionally dividing and frequently becoming vacuolated (Supplementary Fig.3F). To assess whether early ICM cells were more responsive to alternative ESC derivation conditions in a feeder-free environment, we used serum-LIF instead of 2i-LIF under otherwise identical conditions. No ESC colonies emerged from either early (E3.5) or late (E4.5) ICM cells (Supplementary Fig.3G). We also attempted derivations from single-cells in EpiSC conditions (ActivinA plus bFGF), but obtained no pluripotent cell lines (Supplementary Fig.3H).

Isolated ICM cells from the early blastocyst can acquire ERK-independence

The preceding observations indicate that isolated ICM cells of early blastocysts cannot form ESC directly, but acquire competence 6–24 hours later. Proliferation in the presence PD03 is highly selective for pluripotent ESC. We speculated that maturation of early ICM cells may benefit from ERK signalling and that isolated early ICMs may therefore acquire competence to give rise to ESC if allowed to progress *in vitro* in the absence of PD03. To test this, we introduced a 24h ‘maturation’ step into the culture regime. Individual cells were plated in CHIR+LIF or 2i-LIF for 24h. Subsequently, an equal amount of 2i-LIF medium was added and cultures were further propagated in 2i-LIF. Embryos isolated at E3.25-E3.5 are primarily at the early blastocyst stage, but occasionally compacted morulae and expanded blastocysts are included. To avoid the possibility that more advanced, potentially

ESC-competent stages, may contribute to the early embryonic samples, we excluded blastocysts with a cavity occupying more than 50% of the embryo volume (Fig.4a). Samples thus derived are referred to as 'stringent early ICM cells'. Individual cells from these rarely (1%) gave rise to ESC colonies in 2i-LIF (Fig.4b), consistent with our initial observations (Fig.3i). However, when allowed to mature for 24h in CHIR+LIF, the efficiency increased to 12%, comparable to later stages (Fig.4b,e). Expanded ESC lines contributed extensively to chimeras (Fig.4c).

Cells frequently survived in both 2i-LIF and CHIR-LIF (Fig.4d). Thus, the absence of primary ESC colonies emerging from early ICMs in 2i-LIF was unlikely to be attributable to poor cell survival. The recurring presence of large and vacuolated cells (Fig.4f) prompted us to investigate their identity by transcriptional profiling. Applying the modified preamplification method using small groups of cells, we collected 10 vacuolated cells each from the 24h CHIR+LIF (CL), 2i-LIF and CHIR+LIF-matured ESC colonies and assayed them by qRT-PCR. Unsupervised hierarchical clustering with the three lineages of the E4.5 embryo positioned the ESC colony among the epiblast samples, while the vacuolated cells clustered with the trophectoderm (Fig.4g). Further profiling of key trophectodermal markers indicated partial activation of trophoblast-associated genes (Supplementary Fig.4) in vacuolated cells, reminiscent of the fate of singled-mouse blastomeres described recently⁴⁸.

Matrix components support maturation of early ICM cells to Erk-independence

The results above establish that isolated, early ICM cells do not progress to naïve pluripotency when the FGF-Erk signalling cascade is continuously inhibited. However, it has previously been shown that Erk inhibition during preimplantation whole embryo culture results in an increased epiblast compartment at the expense of PrE and supports efficient ESC derivation^{49, 50}. Furthermore, embryos develop into blastocysts with large epiblasts, even when cultured in high concentrations of PD03 (5 μ M compared to 1 μ M in 2i-LIF) from the zygote stage (Fig.5a). This appears inconsistent with the requirement of single-cells to mature without Erk inhibition.

We reasoned that cell-cell or cell-extracellular matrix interactions within the embryo may facilitate progression of ICM cells to an Erk-independent epiblast state. We performed whole-transcriptome analysis by RNA sequencing (RNA-seq) on ICMs of two independent E3.5 blastocysts (insets in Fig.5b) and assessed the expression of major extracellular matrix components (Fig.5b). Strong correlation was observed between biological replicates (Supplementary Fig.5A) and with single-cell datasets produced previously (Supplementary Fig.5B-D)³⁸. We noted minimal expression of collagens, moderate levels of integrins and elevated levels of fibronectin (Fn) and laminins, particularly isoform 511 (Lam511), consisting of Lama5, Lamb1, Lamc1.

Based on this insight we developed an attachment matrix consisting of Fn and recombinant Lam511, which represented approximately half of the extracellular matrix genes expressed at E3.5 in the ICM (Fig.5b'). Fn-Lam511 matrix substantially increased ESC derivation efficiency from single-cells (Fig.5c). We also obtained ESC lines from single early ICM cells with an efficiency of 10%. Nine of thirteen embryos analysed gave rise to at least one ESC colony (Fig.5d). We confirmed this result using stringent early ICM cells

(Supplementary Fig.5E), demonstrating that Fn-Lam511 can bypass the requirement for a maturation step without PD03. The combination of a 24h maturation step in CHIR+LIF and Fn-Lam511 further increased derivation efficiency to 14%. To determine whether the Fn-Lam511 matrix was sufficient to mature early ICM cells, stringent early ICM cells were matured in N2B27 without LIF or inhibitors on Fn-Lam511 (Supplementary Fig.5E) for 24h and subsequently cultured in 2i-LIF. ESC derivation efficiency was 8% from this condition, with two thirds of the embryos giving rise to at least one ESC colony.

To ascertain the specific influence of Lam511 over another isoform, stringent early ICM cells were assayed in parallel on either gelatin, Lam511 or Lam421 in 2i-LIF. Consistent with our previous findings (Fig.5c, Supplementary Fig.5E), Lam511 robustly allowed ESC derivation from single-cells with 11% efficiency, twice that of Lam421 cultures (Fig.5e). Notably, cells attached and initially survived in all of the experimental conditions tested, suggesting a Lam511-specific effect on acquisition of naïve pluripotency.

Given the ability of Fn-Lam511 to promote single-cell ESC line derivation *in vitro*, we determined the localisation of Fn and Lama5 protein by immunofluorescence in the embryo at E3.5 (Fig.5f). Fn was expressed throughout the early blastocyst, while Lama5 was enriched between ICM cells with high Oct4 expression (arrowheads in Fig.5f).

Most preimplantation epiblast cells can give rise to clonal ESC lines

The high efficiency of ESC derivation in 2i-LIF on Fn-Lam511 provided a novel opportunity to explore the potential of each epiblast cell to give rise to an ESC colony. To reduce handling time, we distributed single and small groups of E4.5 ICM cells into one well per embryo of a 4-well plate (Fig.6a). Most late blastocyst ICM cells attached and survived, including PrE cells (Fig.6b). ESC colonies could easily be distinguished from PrE-like cells by morphology, alkaline phosphatase staining (Fig.6a, Supplementary Fig.6A) and lack of *Pdgfra::GFP* marker expression (Fig.6b). Interestingly, PrE-like cells proliferated in 2i-LIF on Fn-Lam511 (arrowhead in Fig.6b) and expressed *Pdgfra::GFP*, Sox17, and variable levels of Gata4 (Supplementary Fig.6B,C), consistent with lineage hierarchy in the embryo⁴⁰. An average of nine ESC colonies per E4.5 embryo was obtained in 2i-LIF using the Fn-Lam511 matrix (Fig.6c). ESC derivation on individual matrix components yielded fewer colonies (Fig.6c). We expanded 12 clonal lines from one embryo from derivations on Fn-Lam511 (FL1-12), 12 from Lam511 (L1-12) and 6 from Fn (F1-6) (Supplementary Fig.6D). Two FL-lines were randomly selected, injected into blastocysts and produced germline chimaeras (Fig.6d).

If all preimplantation epiblast cells have the capacity to give rise to ESC colonies, the cell number in the epiblast should correlate with the number of clonal lines obtained. To test this, we used established protocols to activate and inhibit FGF signalling, resulting in decreased and increased epiblast cell numbers, respectively^{49, 50}. Single-cell ESC derivation from these embryos showed that inhibition of the FGF-MAPK pathway with PD173074 (PD17), a pan-Fgf receptor inhibitor, and PD03 resulted in substantially higher numbers of ESC colonies (average 21 per embryo, and in one instance, 30) compared to DMSO controls (average 5 per embryo) (Fig.6e). In contrast, when embryos were cultured in the presence of Fgf2, PrE-like cells (Supplementary Fig.6E), but no ESC colonies (Fig.6e) were observed. A

direct correlation is evident between the number of ESC colonies and the corresponding published number of epiblast cells for each embryo culture condition (Fig.6f)49–51.

ESC derivation captures preimplantation epiblast cells

Single-cell epiblast culture in defined, feeder-free conditions (2i-LIF on Fn-Lam511) provides a platform to track the process of ESC derivation. To investigate whether ESC colonies originate exclusively from *Pdgfra*-negative epiblast cells, an E4.5 *Pdgfra::GFP* ICM was dissociated into single-cells by repetitive trypsinisation and the cells plated into individual wells. Subsequent time-lapse imaging revealed that all ESC colonies (3/3) arose from GFP-negative epiblast cells (Fig.7a, Supplementary Movie 1). *Pdgfra::GFP*-positive cells were more resistant to single-cell dissociation and generally died after attaching (Fig. 7b). None of the *Pdgfra::GFP*-negative cells transiently activated GFP expression and vice versa, supporting the findings from previous chimera experiments that at E4.5 epiblast and PrE have completed the segregation process^{52, 53}.

The transcriptional and functional similarity of ESC to the preimplantation epiblast led us to analyse the transcriptional dynamics between ICM, epiblast, ESC colonies and established ESC in more detail (Fig.7c). Primary ESC colonies from E4.5 blastocysts were picked at days 2, 4 and 6 of culture. From each colony, 20 cells were randomly collected for preamplification and transcriptional profiling using the 96 gene qRT-PCR array. Early PrE markers expressed in the ICM were downregulated or absent in E4.5 epiblast and ESC (Fig. 7d). In total, 27 of 96 genes were differentially expressed between early ICM and ESC (Supplementary Table 3). In contrast, *Utf1*, *Bmp4* and *Id3* were the only three genes significantly differentially expressed between E4.5 epiblast and ESC (Fig.7e,f, Supplementary Table 3). Expression of naïve pluripotency-associated genes including *Fbxo15*, *Klf2*, *Klf4*, *Nr0b1* and *Zfp42* did not change during ESC derivation (Fig.7g). For a few genes, such as *Klf5*, *Tbx3* and *Dppa3*, we observed dynamic expression during the initial phase of *in vitro* culture. *Tfcp2l1*, *Klf4* and *Esrrb* increased slightly in ESC compared to preimplantation epiblast (Fig.7g, Supplementary Fig.7). Notably, these genes represent direct targets of LIF43, 54, 55 and CHIR56 that stabilise naïve pluripotency and enable ESC self-renewal⁵⁷.

We investigated whether the process of forming primary ESC colonies from single epiblast cells was associated with a distinct transcriptional program. Unsupervised hierarchical clustering unequivocally demonstrated that single-cell ESC derivation and ESC samples remain closest to the E4.5 epiblast (Fig.7h, Supplementary Fig.7B). The ESC samples originated from different mouse strains and derivation media and thus confirmed that the correlation was independent of strain and origin. Moreover, individual derivation time points did not cluster together, suggesting that the cells did not follow a common deviation in expression pattern during the derivation process (Fig.7h).

Finally, we analysed the expression pattern of the naïve pluripotency marker Rex1 by time-lapse microscopy. Our transcriptional analysis showed downregulation of Rex1 (*Zfp42*, Fig. 1c) after implantation, consistent with previous findings⁵⁸. Rex1 was upregulated in the E4.5 epiblast and its expression maintained during ESC derivation (Fig.7g). Time-lapse imaging of single-cell derivation using a destabilised Rex1GFP knock-in reporter mouse²¹

showed that 6/6 ESC colonies originated from Rex1GFP-positive epiblast cells (Fig.7i, Supplementary Movie 2). All colonies exhibited strong Rex1 expression, with 5/6 expressing Rex1 continuously throughout the derivation process in all cells. These experiments indicate that individual epiblast cells can be directly captured in 2i-LIF without traversing distinct developmental states.

Discussion

We have established a fundamental equivalence between *in vitro* cultured ESC and the preimplantation mouse epiblast. Quantitative profiling of 96 genes throughout early embryonic development demonstrated correspondence in the expression of transcription factors and signalling pathway components. Our analysis revealed that early ICM cells are distinct from ESC, with notable differential expression of early PrE-associated genes. In contrast, ESC consistently exhibited the greatest degree of identity to the E4.5 epiblast. A pioneering study carrying out single-cell, whole-transcriptome analysis during the process of ESC derivation has reported that ESC are distinct from E3.5 ICM and E4.5 epiblast³⁸. While this could be attributed partially to the use of feeders and serum-LIF, we noted that the second of the three putative E4.5 epiblast cells analysed by single-cell RNA sequencing most likely belongs to the PrE lineage, given its high levels of PrE markers (including *Gata6*, *Pdgfra*, *Sox17*, *Gata4* and *Sox7*) and 4–18 fold lower expression of epiblast associated genes (including *Nanog*, *Sox2* and *Klf2*; for RNA-seq counts see Table S2 in³⁸). This misassignment may have skewed the average epiblast profile. Here we used *Pdgfra::GFP* reporter mice to distinguish PrE from epiblast. We found the total number of genes differentially expressed between ESC and the embryonic samples to be lowest in the E4.5 epiblast. We cannot rule out that ESC may be even closer to slightly earlier epiblast cells. Unfortunately, technical issues associated with reduced levels of GFP at this stage prevented us from profiling separated epiblast and primitive endoderm progenitors in sufficient numbers from individual embryos at E4.0.

Utf1, *Bmp4* and *Id3* are downregulated in ESC, despite the otherwise robust agreement between cultured lines and E4.5 epiblast. This suggests similar, but not identical transcriptional programs in these cell types. *Bmp* and *Id3* expression were consistently lost within the first two days of derivation, showing that in ground state culture conditions Bmp signalling is not maintained. Conversely, we noted upregulation of direct targets of CHIR and LIF, both of which are present in the culture medium and have been shown to reinforce and stabilise the pluripotency network^{20, 21, 43, 56, 57}.

ESC cultured in serum-LIF were heterogeneous in marker expression and only 1/4 unsorted samples analysed correlated with the preimplantation epiblast. This is consistent with previous reports of ESC heterogeneity^{59–61} and partial differentiation⁶² in this culture regime, and indicates the presence of a proportion of naïve pluripotent cells in serum-LIF, in line with their ability to give rise to chimaeras¹⁴.

The window of development (E3.75-E4.5) from which we consistently generated germline-competent ESC from single ICM cells in stringent 2i-LIF culture conditions correlates with the emergence of epiblast cells in the ICM, a stage also shown to facilitate efficient ESC

derivation of ESC in serum-LIF on feeders⁶³. We also demonstrated that the number of ESC colonies was proportional to epiblast size. Our transcriptional profiling showed that all ESC colonies (15/15) closely paralleled the E4.5 epiblast, supporting the hypothesis that ESC may be captured directly in 2i-LIF⁶⁴ without any requirement for entering a germ cell-like stage, as previously suggested^{65,66}. The absence of expression of *Prdm1* (Blimp1), an early marker of primordial germ cells^{67, 68}, and the sustained expression of *Rex1* observed in primary ESC colonies reinforce this conclusion.

Single-cells from the early blastocyst (E3.25–E3.5) very rarely gave rise to ESC clones in 2i-LIF on gelatin. We show that either withholding PD03 or providing an extracellular matrix imitating the embryonic niche allowed early ICM cells to acquire epiblast identity and competence for self-renewal (Fig.7j). *Lam511*, in combination with serum, has been reported to be sufficient for derivation and self-renewal of ESC⁶⁹. Genetic ablation of laminin genes show severe periimplantation phenotypes: *Lamc1* knockout mice exhibit defects in segregation of epiblast and PrE and arrest at E5.5⁷⁰. *Lamb1*-deficient embryos also die soon after implantation⁷¹. We show by RNA sequencing that *Lam511* is expressed in the early ICM, as is $\beta 1$ -*integrin*, which mediates laminin binding in ESC^{69, 73}. Genetic deletion of $\beta 1$ -*integrin* causes complete loss of epiblast at E5.5⁷². A potential candidate pathway downstream of integrin signalling could be PI3K⁷³. The PI3K subunit p110 β was shown to be essential for preimplantation development⁷⁴. Further studies are required to delineate the essential downstream pathways mediating the transition from ICM to epiblast in the early embryo.

The average number of epiblast cells in mid- to late-blastocysts is between 10 and 2040. We derived on average 9 clonal ESC lines per E4.5 embryo. Allowing for cell lysis during single-cell manipulation, incomplete dissociation of the ICM compartment and imperfect cloning efficiency, as encountered even with established ESC²¹, our results indicate that most, if not all, preimplantation epiblast cells can give rise to naïve pluripotent ESC. This efficient and direct transition underscores the intrinsic similarity of ESC to the preimplantation epiblast. We therefore propose that the ESC ground state is defined medium is directly derived from, and retains all essential features of naïve pluripotent epiblast cells as they first emerge in the embryo.

Materials and Methods

Experimental procedures are described in Supplementary Materials and Methods.

Supplementary Material

Refer to Web version on PubMed Central for supplementary material.

Acknowledgments

We thank Charles-Étienne Dumeau and William Mansfield for chimaera production, Peter Humphreys for assistance with imaging, Samuel Jameson and staff for animal husbandry, the EMBL Genomics Core Facility for sequencing, and Graziano Martello for helpful discussion on the manuscript. This work was supported by funding from the Wellcome Trust, Medical Research Council, BBSRC, the Louis Jeantet Foundation, EMBL and the University of Cambridge. Austin Smith is a Medical Research Council Professor.

References

1. Nichols J, et al. Formation of pluripotent stem cells in the mammalian embryo depends on the POU transcription factor Oct4. *Cell*. 1998; 95:379–391. [PubMed: 9814708]
2. Chambers I, et al. Functional expression cloning of Nanog, a pluripotency sustaining factor in embryonic stem cells. *Cell*. 2003; 113:643–655. [PubMed: 12787505]
3. Kurimoto K, et al. An improved single-cell cDNA amplification method for efficient high-density oligonucleotide microarray analysis. *Nucleic Acids Res*. 2006; 34:e42. [PubMed: 16547197]
4. Guo G, et al. Resolution of cell fate decisions revealed by single-cell gene expression analysis from zygote to blastocyst. *Dev Cell*. 2010; 18:675–685. [PubMed: 20412781]
5. Avilion AA, et al. Multipotent cell lineages in early mouse development depend on SOX2 function. *Genes Dev*. 2003; 17:126–140. [PubMed: 12514105]
6. Artus J, Piliszek A, Hadjantonakis AK. The primitive endoderm lineage of the mouse blastocyst: sequential transcription factor activation and regulation of differentiation by Sox17. *Dev Biol*. 2011; 350:393–404. [PubMed: 21146513]
7. Frankenberg S, et al. Primitive endoderm differentiates via a three-step mechanism involving Nanog and RTK signaling. *Dev Cell*. 2011; 21:1005–1013. [PubMed: 22172669]
8. Chazaud C, Yamanaka Y, Pawson T, Rossant J. Early lineage segregation between epiblast and primitive endoderm in mouse blastocysts through the Grb2-MAPK pathway. *Dev Cell*. 2006; 10:615–624. [PubMed: 16678776]
9. Morrissey EE, et al. GATA6 regulates HNF4 and is required for differentiation of visceral endoderm in the mouse embryo. *Genes Dev*. 1998; 12:3579–3590. [PubMed: 9832509]
10. Niakan KK, et al. Sox17 promotes differentiation in mouse embryonic stem cells by directly regulating extraembryonic gene expression and indirectly antagonizing self-renewal. *Genes Dev*. 2010; 24:312–326. [PubMed: 20123909]
11. Koutsourakis M, Langeveld A, Patient R, Beddington R, Grosveld F. The transcription factor GATA6 is essential for early extraembryonic development. *Development*. 1999; 126:723–732.
12. Evans MJ, Kaufman MH. Establishment in culture of pluripotential cells from mouse embryos. *Nature*. 1981; 292:154–156. [PubMed: 7242681]
13. Martin GR. Isolation of a pluripotent cell line from early mouse embryos cultured in medium conditioned by teratocarcinoma stem cells. *Proc Natl Acad Sci U S A*. 1981; 78:7634–7638. [PubMed: 6950406]
14. Williams RL, et al. Myeloid leukaemia inhibitory factor maintains the developmental potential of embryonic stem cells. *Nature*. 1988; 336:684–687. [PubMed: 3143916]
15. Smith AG, et al. Inhibition of pluripotential embryonic stem cell differentiation by purified polypeptides. *Nature*. 1988; 336:688–690. [PubMed: 3143917]
16. Silva J, Smith A. Capturing pluripotency. *Cell*. 2008; 132:532–536. [PubMed: 18295569]
17. Nichols J, Smith A. Naive and primed pluripotent states. *Cell Stem Cell*. 2009; 4:487–492. [PubMed: 19497275]
18. Kunath T, et al. FGF stimulation of the Erk1/2 signalling cascade triggers transition of pluripotent embryonic stem cells from self-renewal to lineage commitment. *Development*. 2007; 134:2895–2902. [PubMed: 17660198]
19. Burdon T, Stracey C, Chambers I, Nichols J, Smith A. Suppression of SHP-2 and ERK signalling promotes self-renewal of mouse embryonic stem cells. *Dev Biol*. 1999; 210:30–43. [PubMed: 10364425]
20. Ying QL, et al. The ground state of embryonic stem cell self-renewal. *Nature*. 2008; 453:519–523. [PubMed: 18497825]
21. Wray J, et al. Inhibition of glycogen synthase kinase-3 alleviates Tcf3 repression of the pluripotency network and increases embryonic stem cell resistance to differentiation. *Nat Cell Biol*. 2011; 13:838–845. [PubMed: 21685889]
22. Brons IG, et al. Derivation of pluripotent epiblast stem cells from mammalian embryos. *Nature*. 2007; 448:191–195. [PubMed: 17597762]

23. Tesar PJ, et al. New cell lines from mouse epiblast share defining features with human embryonic stem cells. *Nature*. 2007; 448:196–199. [PubMed: 17597760]
24. Guo G, et al. Klf4 reverts developmentally programmed restriction of ground state pluripotency. *Development*. 2009; 136:1063–1069. [PubMed: 19224983]
25. Silva J, et al. Promotion of reprogramming to ground state pluripotency by signal inhibition. *PLoS Biol*. 2008; 6:e253. [PubMed: 18942890]
26. Theunissen TW, et al. Nanog overcomes reprogramming barriers and induces pluripotency in minimal conditions. *Curr Biol*. 2011; 21:65–71. [PubMed: 21194951]
27. Nichols J, et al. Validated germline-competent embryonic stem cell lines from nonobese diabetic mice. *Nat Med*. 2009; 15:814–818. [PubMed: 19491843]
28. Hanna J, et al. Metastable pluripotent states in NOD-mouse-derived ESCs. *Cell Stem Cell*. 2009; 4:513–524. [PubMed: 19427283]
29. Buehr M, et al. Capture of authentic embryonic stem cells from rat blastocysts. *Cell*. 2008; 135:1287–1298. [PubMed: 19109897]
30. Li P, et al. Germline competent embryonic stem cells derived from rat blastocysts. *Cell*. 2008; 135:1299–1310. [PubMed: 19109898]
31. Tesar PJ. Derivation of germ-line-competent embryonic stem cell lines from preblastocyst mouse embryos. *Proc Natl Acad Sci U S A*. 2005; 102:8239–8244. [PubMed: 15917331]
32. Delhaise F, Bralio V, Schuurbiens N, Dessy F. Establishment of an embryonic stem cell line from 8-cell stage mouse embryos. *Eur J Morphol*. 1996; 34:237–243. [PubMed: 8982633]
33. Chung Y, et al. Embryonic and extraembryonic stem cell lines derived from single mouse blastomeres. *Nature*. 2006; 439:216–219. [PubMed: 16227970]
34. Wakayama S, et al. Efficient establishment of mouse embryonic stem cell lines from single blastomeres and polar bodies. *Stem Cells*. 2007; 25:986–993. [PubMed: 17185608]
35. Bao S, et al. Epigenetic reversion of post-implantation epiblast to pluripotent embryonic stem cells. *Nature*. 2009; 461:1292–1295. [PubMed: 19816418]
36. Macfarlan TS, et al. Embryonic stem cell potency fluctuates with endogenous retrovirus activity. *Nature*. 2012; 487:57–63. [PubMed: 22722858]
37. Tang F, et al. RNA-Seq analysis to capture the transcriptome landscape of a single-cell. *Nat Protoc*. 2010; 5:516–535. [PubMed: 20203668]
38. Tang F, et al. Tracing the derivation of embryonic stem cells from the inner cell mass by single-cell RNA-Seq analysis. *Cell Stem Cell*. 2010; 6:468–478. [PubMed: 20452321]
39. Solter D, Knowles BB. Immunosurgery of mouse blastocyst. *Proc Natl Acad Sci U S A*. 1975; 72:5099–5102. [PubMed: 1108013]
40. Plusa B, Piliszek A, Frankenberg S, Artus J, Hadjantonakis AK. Distinct sequential cell behaviours direct primitive endoderm formation in the mouse blastocyst. *Development*. 2008; 135:3081–3091. [PubMed: 18725515]
41. Hamilton TG, Klinghoffer RA, Corrin PD, Soriano P. Evolutionary divergence of platelet-derived growth factor alpha receptor signaling mechanisms. *Mol Cell Biol*. 2003; 23:4013–4025. [PubMed: 12748302]
42. He B, et al. Cloning and characterization of a functional promoter of the human SOCS-3 gene. *Biochem Biophys Res Commun*. 2003; 301:386–391. [PubMed: 12565872]
43. Bourillot PY, et al. Novel STAT3 target genes exert distinct roles in the inhibition of mesoderm and endoderm differentiation in cooperation with Nanog. *Stem Cells*. 2009; 27:1760–1771. [PubMed: 19544440]
44. Coucouvanis E, Martin GR. BMP signaling plays a role in visceral endoderm differentiation and cavitation in the early mouse embryo. *Development*. 1999; 126:535–546. [PubMed: 9876182]
45. Guzman-Ayala M, et al. Graded Smad2/3 activation is converted directly into levels of target gene expression in embryonic stem cells. *PLoS One*. 2009; 4:e4268. [PubMed: 19172185]
46. Marks H, et al. The transcriptional and epigenomic foundations of ground state pluripotency. *Cell*. 2012; 149:590–604. [PubMed: 22541430]
47. Wray J, Kalkan T, Smith AG. The ground state of pluripotency. *Biochem Soc Trans*. 2010; 38:1027–1032. [PubMed: 20658998]

48. Lorthongpanich C, Doris TP, Limviphuvadh V, Knowles BB, Solter D. Developmental fate and lineage commitment of singled mouse blastomeres. *Development*. 2012; 139:3722–3731. [PubMed: 22991438]
49. Nichols J, Silva J, Roode M, Smith A. Suppression of Erk signalling promotes ground state pluripotency in the mouse embryo. *Development*. 2009; 136:3215–3222. [PubMed: 19710168]
50. Yamanaka Y, Lanner F, Rossant J. FGF signal-dependent segregation of primitive endoderm and epiblast in the mouse blastocyst. *Development*. 2010; 137:715–724. [PubMed: 20147376]
51. Roode M, et al. Human hypoblast formation is not dependent on FGF signalling. *Dev Biol*. 2012; 361:358–363. [PubMed: 22079695]
52. Grabarek JB, et al. Differential plasticity of epiblast and primitive endoderm precursors within the ICM of the early mouse embryo. *Development*. 2012; 139:129–139. [PubMed: 22096072]
53. Gardner RL, Rossant J. Investigation of the fate of 4-5 day post-coitum mouse inner cell mass cells by blastocyst injection. *J Embryol Exp Morphol*. 1979; 52:141–152. [PubMed: 521746]
54. Hall J, et al. Oct4 and LIF/Stat3 additively induce Kruppel factors to sustain embryonic stem cell self-renewal. *Cell Stem Cell*. 2009; 5:597–609. [PubMed: 19951688]
55. Martello G, et al. Identification of the Missing Pluripotency Factor Downstream of Leukaemia Inhibitory Factor. *EMBO J*. 2013
56. Martello G, et al. Esrrb is a pivotal target of the Gsk3/Tcf3 axis regulating embryonic stem cell self-renewal. *Cell Stem Cell*. 2012; 11:491–504. [PubMed: 23040478]
57. Nichols J, Smith A. Pluripotency in the embryo and in culture. *Cold Spring Harb Perspect Biol*. 2012; 4:a008128. [PubMed: 22855723]
58. Pelton TA, Sharma S, Schulz TC, Rathjen J, Rathjen PD. Transient pluripotent cell populations during primitive ectoderm formation: correlation of in vivo and in vitro pluripotent cell development. *J Cell Sci*. 2002; 115:329–339. [PubMed: 11839785]
59. Chambers I, et al. Nanog safeguards pluripotency and mediates germline development. *Nature*. 2007; 450:1230–1234. [PubMed: 18097409]
60. Hayashi K, Lopes SM, Tang F, Surani MA. Dynamic equilibrium and heterogeneity of mouse pluripotent stem cells with distinct functional and epigenetic states. *Cell Stem Cell*. 2008; 3:391–401. [PubMed: 18940731]
61. Toyooka Y, Shimosato D, Murakami K, Takahashi K, Niwa H. Identification and characterization of subpopulations in undifferentiated ES cell culture. *Development*. 2008; 135:909–918. [PubMed: 18263842]
62. Smith A. Nanog heterogeneity: tilting at windmills? *Cell Stem Cell*. 2013; 13:6–7. [PubMed: 23827703]
63. Brook FA, Gardner RL. The origin and efficient derivation of embryonic stem cells in the mouse. *Proc Natl Acad Sci U S A*. 1997; 94:5709–5712. [PubMed: 9159137]
64. Nichols J, Smith A. The origin and identity of embryonic stem cells. *Development*. 2011; 138:3–8. [PubMed: 21138972]
65. Zwaka TP, Thomson JA. A germ cell origin of embryonic stem cells? *Development*. 2005; 132:227–233. [PubMed: 15623802]
66. Chu LF, Surani MA, Jaenisch R, Zwaka TP. Blimp1 expression predicts embryonic stem cell development in vitro. *Curr Biol*. 2011; 21:1759–1765. [PubMed: 22000107]
67. Ohinata Y, et al. Blimp1 is a critical determinant of the germ cell lineage in mice. *Nature*. 2005; 436:207–213. [PubMed: 15937476]
68. Vincent SD, et al. The zinc finger transcriptional repressor Blimp1/Prdm1 is dispensable for early axis formation but is required for specification of primordial germ cells in the mouse. *Development*. 2005; 132:1315–1325. [PubMed: 15750184]
69. Domogatskaya A, Rodin S, Boutaud A, Tryggvason K. Laminin-511 but not -332, -111, or -411 enables mouse embryonic stem cell self-renewal in vitro. *Stem Cells*. 2008; 26:2800–2809. [PubMed: 18757303]
70. Smyth N, et al. Absence of basement membranes after targeting the LAMC1 gene results in embryonic lethality due to failure of endoderm differentiation. *J Cell Biol*. 1999; 144:151–160. [PubMed: 9885251]

71. Miner JH, Li C, Mudd JL, Go G, Sutherland AE. Compositional and structural requirements for laminin and basement membranes during mouse embryo implantation and gastrulation. *Development*. 2004; 131:2247–2256. [PubMed: 15102706]
72. Fassler R, Meyer M. Consequences of lack of beta 1 integrin gene expression in mice. *Genes Dev*. 1995; 9:1896–1908. [PubMed: 7544313]
73. Keely PJ. Mechanisms by which the extracellular matrix and integrin signaling act to regulate the switch between tumor suppression and tumor promotion. *J Mammary Gland Biol Neoplasia*. 2011; 16:205–219. [PubMed: 21822945]
74. Bi L, Okabe I, Bernard DJ, Nussbaum RL. Early embryonic lethality in mice deficient in the p110beta catalytic subunit of PI 3-kinase. *Mamm Genome*. 2002; 13:169–172. [PubMed: 11919689]
75. Hooper M, Hardy K, Handyside A, Hunter S, Monk M. HPRT-deficient (Lesch-Nyhan) mouse embryos derived from germline colonization by cultured cells. *Nature*. 1987; 326:292–295. [PubMed: 3821905]
76. Haapa-Paananen S, et al. HES6 gene is selectively overexpressed in glioma and represents an important transcriptional regulator of glioma proliferation. *Oncogene*. 2012; 31:1299–1310. [PubMed: 21785461]
77. Tang F, et al. mRNA-Seq whole-transcriptome analysis of a single-cell. *Nat Methods*. 2009; 6:377–382. [PubMed: 19349980]
78. Dvinge H, Bertone P. HTqPCR: high-throughput analysis and visualization of quantitative real-time PCR data in R. *Bioinformatics*. 2009; 25:3325–3326. [PubMed: 19808880]
79. Mamo S, Gal AB, Bodo S, Dinnyes A. Quantitative evaluation and selection of reference genes in mouse oocytes and embryos cultured in vivo and in vitro. *BMC Dev Biol*. 2007; 7:14. [PubMed: 17341302]
80. Aird D, et al. Analyzing and minimizing PCR amplification bias in Illumina sequencing libraries. *Genome Biol*. 2011; 12:R18. [PubMed: 21338519]
81. Wu TD, Nacu S. Fast and SNP-tolerant detection of complex variants and splicing in short reads. *Bioinformatics*. 2010; 26:873–881. [PubMed: 20147302]
82. Flicek P, et al. Ensembl 2013. *Nucleic Acids Res*. 2013; 41:D48–55. [PubMed: 23203987]

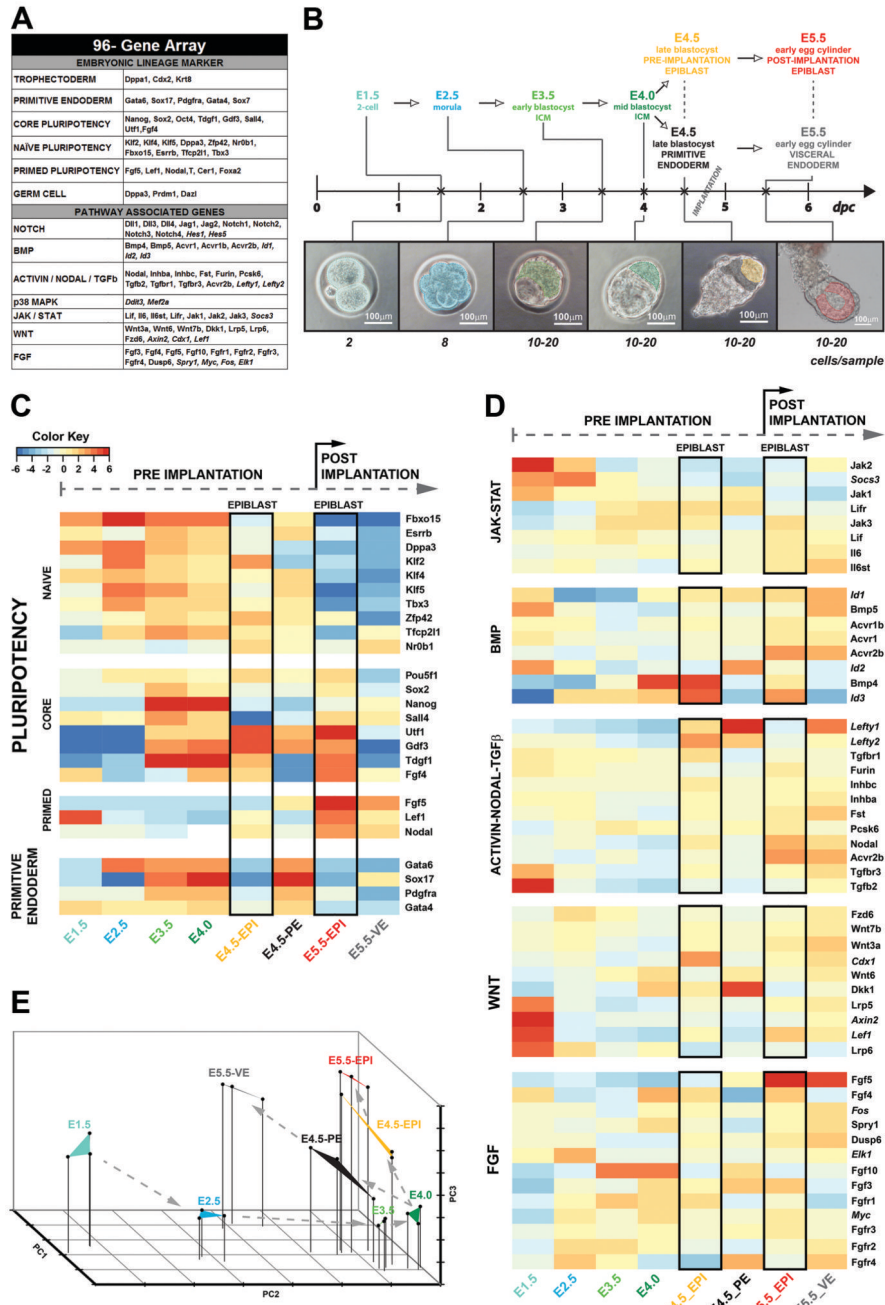


Figure 1. Gene expression in early mouse development

(A) Lineage markers and pathway-associated genes assayed by qRT-PCR array (downstream targets in italic). (B) Summary of the embryonic lineages profiled. Three embryos were analysed per developmental stage with the first shown in the figure. The embryonic lineages isolated are shown in pseudocolours, with the approximate numbers of cells for expression profiling underneath. (C) Lineage markers normalised to mean expression value. (D) Expression of Jak-Stat, Bmp, Activin-Nodal-Tgfb, Wnt and Fgf signalling pathway-associated genes with downstream targets in italics. (E) PCA of embryonic samples from

E1.5-5.5 based on qRT-PCR arrays. All data points represent independent biological replicates. Triangles between data points are drawn based on the corresponding developmental stage.

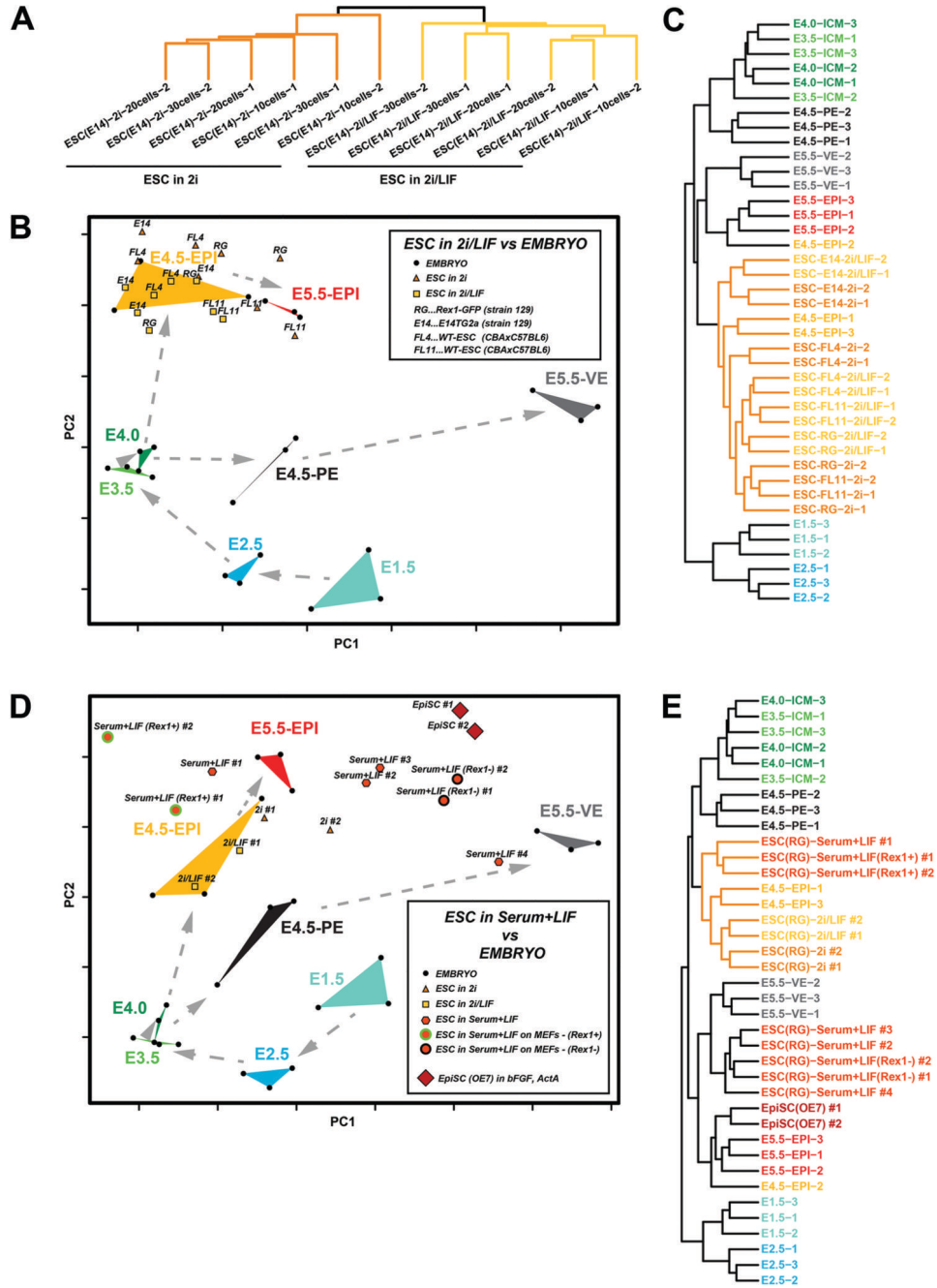


Figure 2. Correlation of ESC gene expression to the early embryo
 (A) Hierarchical clustering of ESC samples from 10, 20 and 30 cells cultured in 2i and 2i-LIF. (B) PCA of embryonic stages and ESC samples obtained from 2i and 2i-LIF cultures on gelatin. Two independent biological replicates, each containing 20 randomly picked cells of the 4 ESC lines indicated in the graph, for both 2i and 2i-LIF, were processed and profiled by qRT-PCR arrays. (C) Hierarchical clustering of the data set shown in B. The major cluster containing ESC samples in 2i and 2i-LIF is highlighted in orange. (D) PCA of embryonic stages, ESC samples cultured in serum-LIF on gelatin or feeders and EpiSC maintained on

fibronectin. Two independent biological replicates, each containing 20 randomly-picked cells, were processed and profiled by qRT-PCR arrays for each experimental condition. (E) Hierarchical clustering of the data set shown in D. ESC samples clustering close to the E4.5 epiblast are highlighted in orange.

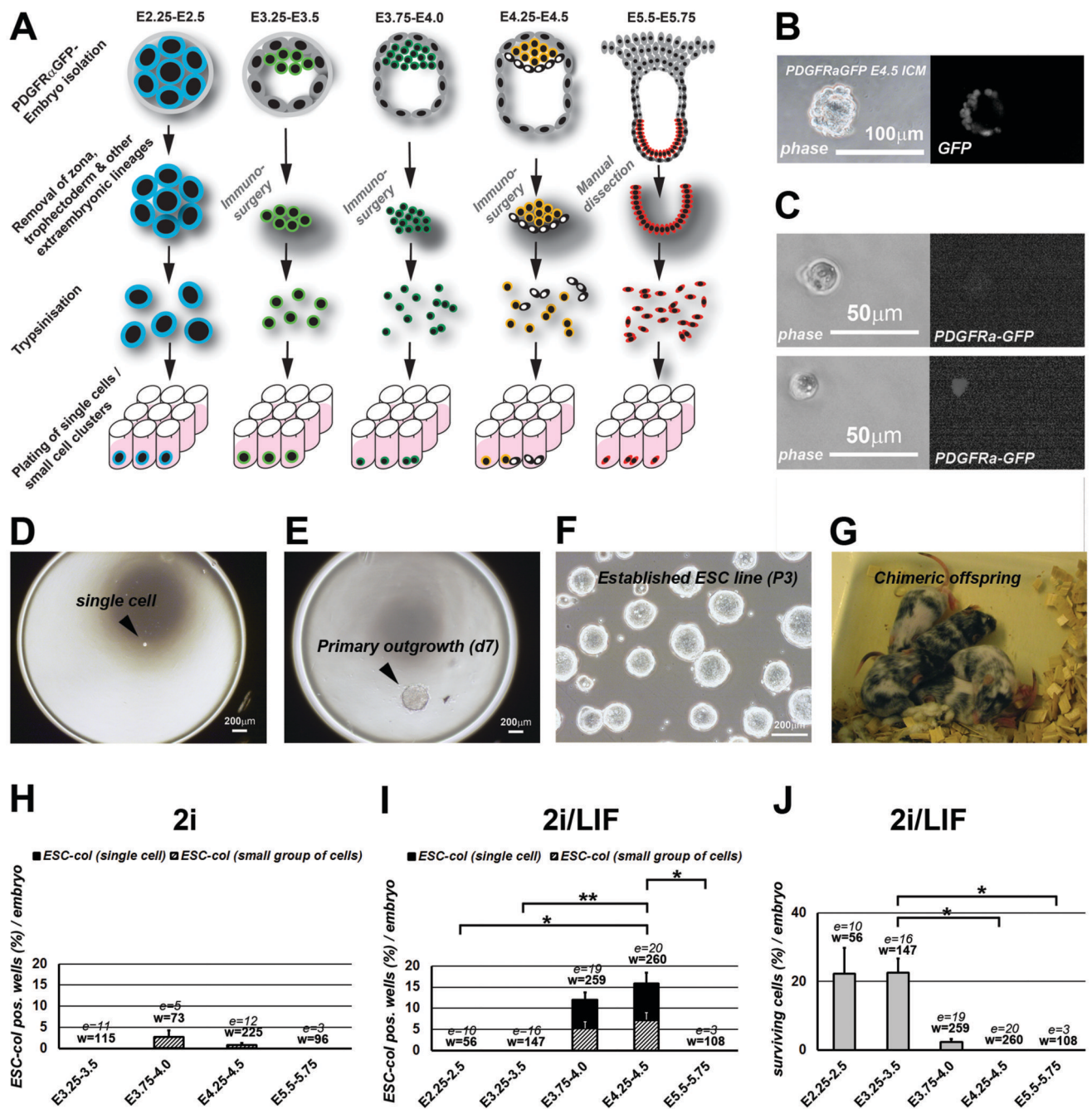


Figure 3. Functional analysis of embryonic cells by single-cell ESC derivation

(A) Schematic outline of the single-cell ESC derivation assay in a fully defined system using embryos from *Pdgfra::GFP* F1 crosses. (B) Image of an isolated ICM after immunosurgery of an E4.5 embryo with *Pdgfra::GFP* expression in PrE. (C) Dissociated single presumptive epiblast cell (upper panel) and a presumptive PrE cell (lower panel). (D-G) ESC derivation process: an isolated embryonic cell is plated into an individual well (D), grows to an ESC colony within 7 days (E) and is expanded into an ESC line (F) with high chimeric contribution (G). Representative images in B-G, more than 20 replicates. (H-I) Single-cell

ESC derivation efficiency in 2i (H) and 2i-LIF (I). Efficiency is displayed as the percentage of ESC-colony positive wells per embryo (ESC-col. pos. wells (%)/embryo) after 7 days. The total efficiency is further subdivided into ESC colonies arising from truly individual cells (ESC-col (single-cell)) and ESC arising from small groups, usually between 2-5 cells (ESC-col (small group of cells)). $*=P<0.05$, $**=P<0.01$ as determined by one-way ANOVA with subsequent Tukey HSD testing. The graphs show the mean and S.E.M. for the percentage of ESC colony-containing wells per embryo resulting from the analysis of $n='e'$ embryos (with at least 3 wells analysed per embryo for each time point of embryonic development shown on the X axis, 'w' represents the total number of wells analysed per time point). Embryos were obtained from at least 3 individual litters on at least 3 different days. (J) Percentage of wells containing at least one surviving cell by morphology after 7 days per embryo in 2i-LIF; e =number of embryos analysed, w =number of wells analysed, $*=P<0.05$ as determined by One-way ANOVA with subsequent Tukey HSD testing. The graph shows the mean and S.E.M. for the percentage of surviving cell-containing wells per embryo resulting from the analysis of $n='e'$ embryos (with at least 3 wells analysed per embryo for each time point of embryonic development shown on the X axis, 'w' represents the total number of wells analysed per time point). Embryos were obtained from at least 3 individual litters on at least 3 different days.

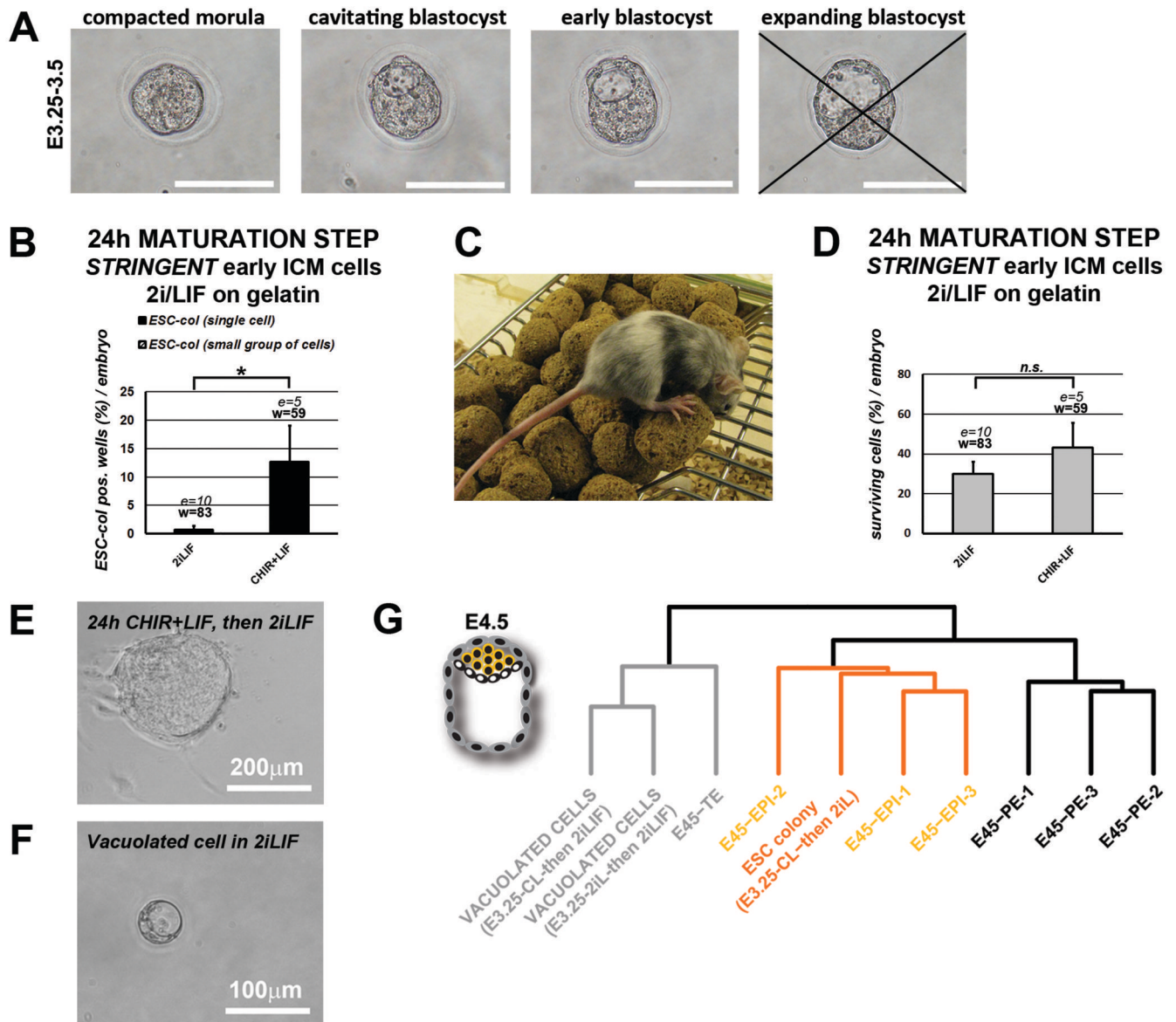


Figure 4. Maturation in the absence of MEK inhibition allows individual ICM cell acquisition of naïve pluripotency

(A) Embryos obtained after uterine flush at E3.5. For “stringent early ICM cells” expanding blastocyst stages with more than 50% cavity volume were excluded. Scale bar = 200 μm. (B) Single-cell ESC derivation efficiency in percentage of ESC-colony positive wells per embryo (ESC-col. pos. wells (%) / embryo) of stringent early E3.5 ICM cells. For the 24h maturation step, single-cells were cultured for the first day in the medium condition indicated and on the second day an equal amount of 2i-LIF was added. Subsequently the cultures were maintained in 2i-LIF. * = $P < 0.05$ as determined by Student’s two tailed t-test. The graph shows the mean and S.E.M. for the percentage of ESC colony-containing wells per embryo resulting from the analysis of $n = e$ embryos (with at least 4 wells analysed per embryo for each experimental condition shown on the X axis, ‘w’ represents the total number of wells analysed per experimental condition). Embryos were obtained from at least

3 individual litters on two different days. (C) Chimeric mouse obtained from injecting cells of a day 6 ESC colony into a host blastocyst. The ESC colony was derived from a single, stringent early E3.5 ICM cell including a 24h maturation step in CHIR+LIF. (D) Surviving cells by morphology after 7 days in percentage of wells per embryo, as described in (B). Error bars are S.E.M. calculated from the percentage of wells containing surviving cells per embryo resulting from the analysis of $n='e'$ embryos (with at least 4 wells analysed per embryo for each experimental condition shown on the X axis, 'w' represents the total number of wells analysed per experimental condition). (E) ESC colony derived from an individual stringent early E3.5 ICM cell after 24h CHIR+LIF incubation. (F) Vacuolated, surviving cell which did not develop into an ESC colony. Representative images in E and F, more than 5 replicates. (G) Schematic of an E4.5 embryo and hierarchical clustering of an ESC colony obtained including a 24h maturation step in CHIR+LIF, 10 vacuolated cells obtained including a 24h maturation step in CHIR+LIF and 10 vacuolated cells obtained in 2i-LIF cultures only from stringent early E3.5 ICM cells, three E4.5 epiblast, three E4.5 PrE and one E4.5 trophectoderm sample.

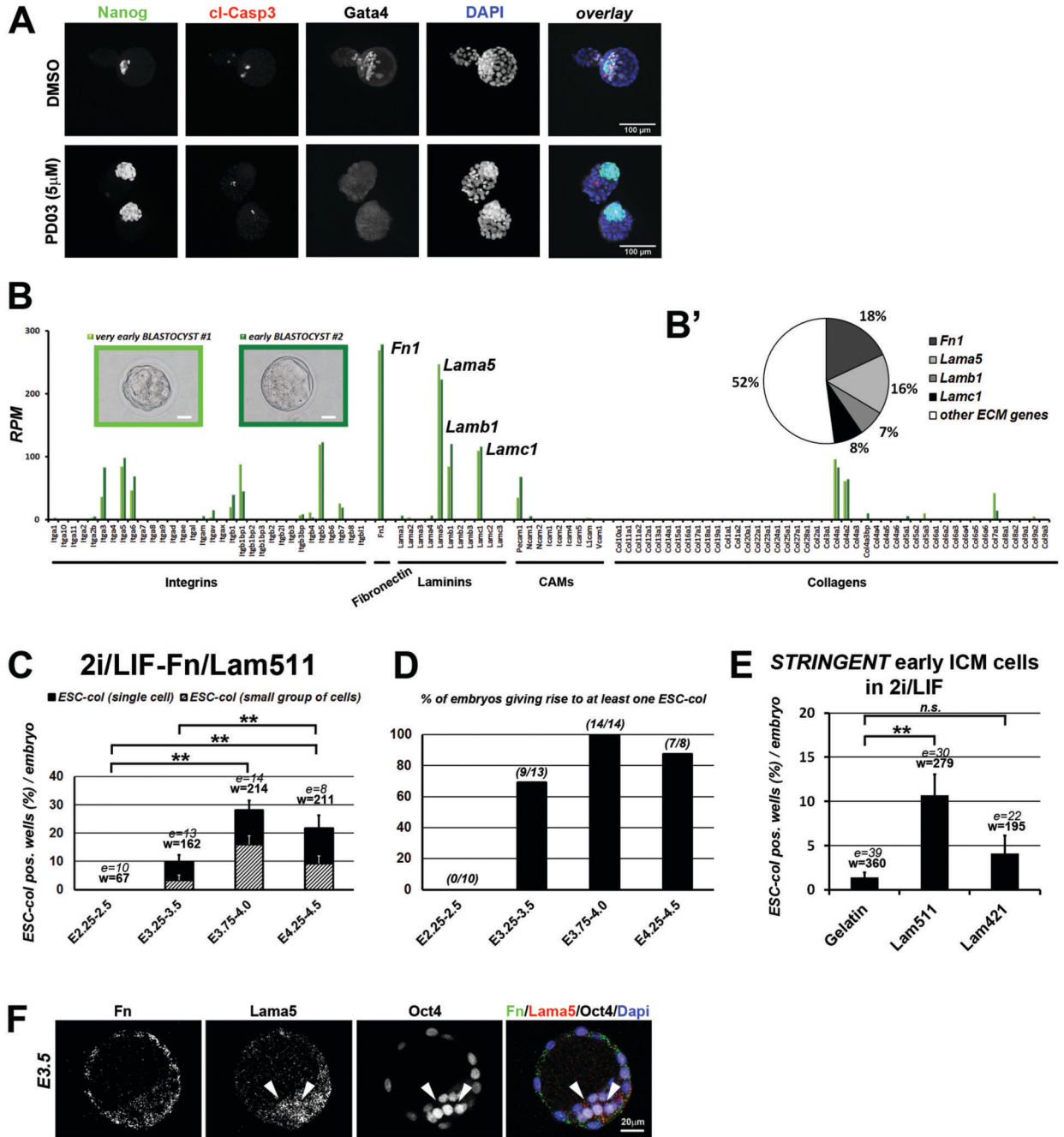


Figure 5. Components of the embryonic extracellular matrix allow ESC derivation in the presence of PD03 from individual early ICM cells
 (A) Immunofluorescence staining of blastocysts cultured *in vitro* from the zygote in the presence of either DMSO or 5µM PD03. Representative images, more than 3 replicates. (B) RNA levels in RPM (mapped reads per million base pairs sequenced) for two early blastocysts (insets, scale bar=50µm) of major extracellular matrix genes. B' represents the percentage of RNA levels of Fn1 and Lama5, Lamb1, Lamc1 over the remaining extracellular matrix genes displayed in B. (C) Single-cell ESC derivation efficiency in 2i-LIF on Fn-Lam511. Efficiency is displayed as the percentage of ESC-colony positive wells

per embryo (ESC-col. pos. wells(%) / embryo) after 7 days. The total efficiency is further subdivided into ESC colonies arising from truly individual cells (ESC-col (single-cell)) and ESC arising from small groups, usually between 2-5 cells (ESC-col (small group of cells)). $**=P<0.01$ as determined by One-way ANOVA with subsequent Tukey HSD testing. The graph shows the mean and S.E.M. for the percentage of ESC colony-containing wells per embryo resulting from the analysis of $n='e'$ embryos (with at least 4 wells analysed per embryo for each time point of embryonic development shown on the X axis, 'w' represents the total number of wells analysed per time point). Embryos were obtained from at least 3 individual litters on at least 3 different days. (D) Percentage of embryos giving rise to at least one ESC colony in 2i-LIF on Fn-Lam511. The numbers of embryos yielding at least one ESC colony per total number of embryos analysed are indicated. (E) Single-cell ESC derivation efficiencies of stringent early ICM cells in 2i-LIF on the substrates indicated, as described in (C). The graph shows the mean and S.E.M. for the percentage of ESC colony-containing wells per embryo resulting from the analysis of $n='e'$ embryos (with at least 4 wells analysed per embryo for each experimental condition shown on the X axis, 'w' represents the total number of wells analysed per experimental condition). (F) Immunofluorescence staining of a E3.5 blastocyst for Fn, Lama5 and Oct4. Representative images, more than 3 replicates.

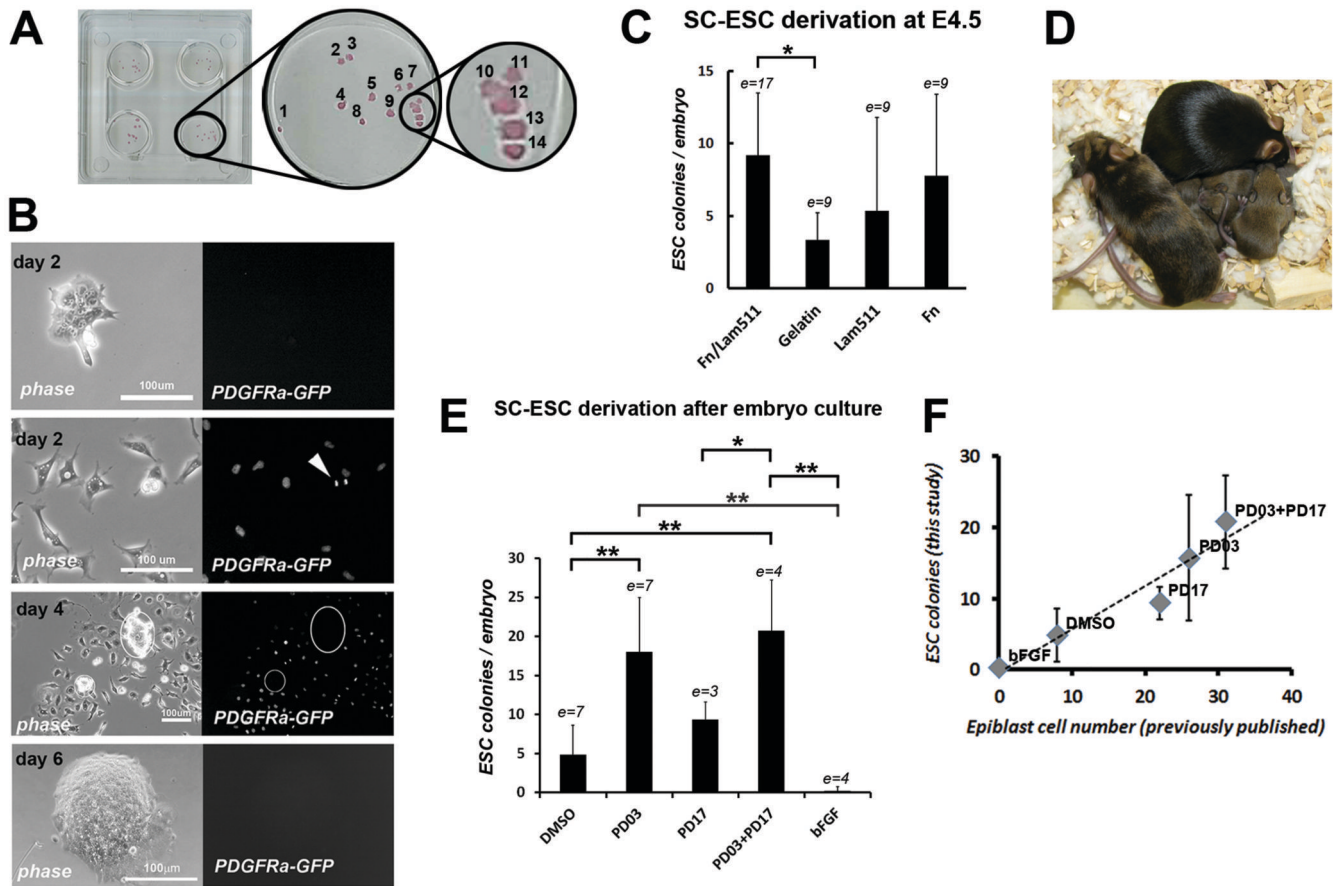


Figure 6. Maximising the number of clonal ESC lines derived from the preimplantation epiblast (A) Alkaline phosphatase staining of ESC colonies after single-cell ESC derivation in 2i-LIF on Fn-Lam511 at day 7. An E4.5 ICM was trypsinised and single as well as small groups of cells were evenly distributed with a mouth pipette. Representative images, more than 10 replicates. (B) Representative images of day 2, 4 and 6 after single-cell ESC derivation as described in A. (C) Total number of ESC colonies per E4.5 embryo at day 7 on the substrates indicated; e=number of embryos analysed, $*=P<0.05$ as determined by One-way ANOVA with subsequent Tukey HSD testing. Error bars are S.D. calculated from the number of ESC colonies per embryo. Embryos were obtained from at least 2 individual litters on at least 3 different days. (D) Germline transmission of a clonal ESC line derived on Fn-Lam511. (E) Total number of ESC colonies per embryo after culture from the 8-cell stage for three days in the presence of activators or inhibitors of FGF signalling; ‘n’ values are expressed as ‘e’=number of embryos analysed, $**=P<0.01$, $*=P<0.05$ as determined by One-way ANOVA with subsequent Tukey HSD testing. Error bars are S.D. calculated from the number of ESC colonies per embryo. Embryos were obtained from at least 2 individual litters on at least 3 different days. (F) Correlation plot of ESC colonies shown in E with the number of Nanog-positive epiblast cells reported for the embryo culture conditions indicated. Error bars are S.D. as described in (E). The corresponding references are: bFGF50, DMSO, PD17 and PD03 49 and PD03+PD17 51.

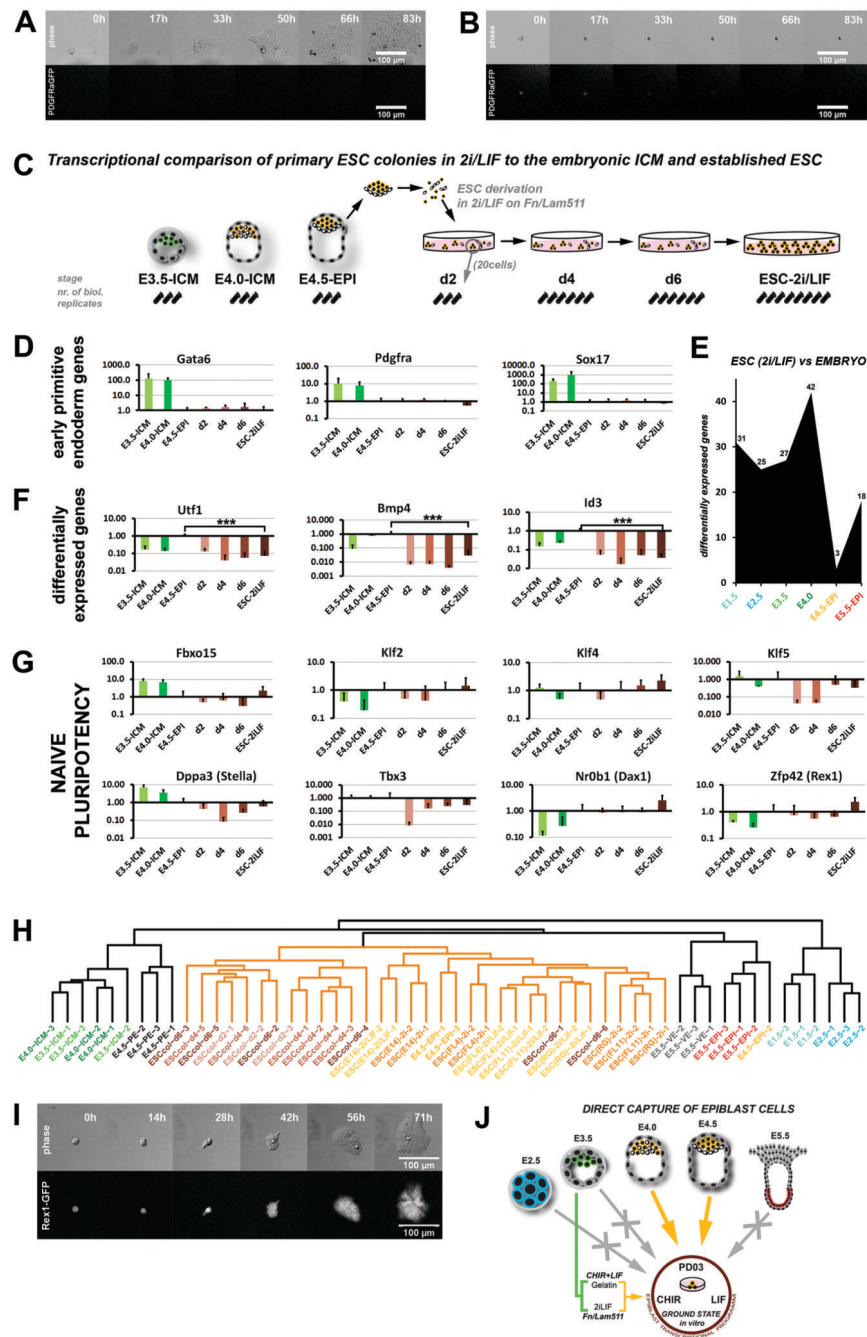


Figure 7. ESC colonies are directly captured in a transcriptional state closest to the E4.5 epiblast (A-B) Time-lapse of ESC derivation using the *Pdgfra::GFP* reporter line in 2i-LIF on Fn-Lam511 at E4.5. Following immunosurgery the ICM was rendered into a single-cell suspension by repetitive trypsinisation, and cells were deposited into individual wells. Clonal ESC colonies arose exclusively from *Pdgfra::GFP* negative cells (A), but not *Pdgfra::GFP* positive cells (B). (C) Schematic representation of embryonic stages and sample acquisition for gene expression analysis during ESC derivation. Primary ESC colonies were derived by manual plating of dissociated E4.5 ICMs on Fn-Lam511 in 2i-LIF.

For each biological replicate, one colony was manually picked, trypsinised and 20 randomly-selected cells were used for cDNA preamplification and transcriptional analysis by 96 gene RT-qPCR at days 2, 4 and 6. (D,F,G) Direct comparison of RNA levels in embryonic samples E3.5-ICM, E4.0-ICM and E4.5-EPI (epiblast), ESC derivation samples day 2-6 and established ESC in 2i-LIF (average of the 4 lines analysed in this study: E14, RG, FL4 and FL11). Expression levels are shown relative to the preimplantation epiblast (E4.5-EPI) on a logarithmic scale for (D) PrE markers, (F) significantly downregulated genes between ESC and E4.5 epiblast, ***= $P < 0.001$ as determined by Student's two tailed t-test corrected for multiple testing using the Benjamini-Hochberg procedure, and (G) naïve pluripotency markers. Error bars are S.D. between biological replicates. The number of independent biological replicates is indicated in C. (E) Graph showing the total number of significantly differentially ($P < 0.05$) expressed genes of ESC compared to the indicated embryonic stages. (H) Unbiased hierarchical clustering of primary ESC colonies at derivation day 2, 4 and 6 in 2i-LIF on Fn-Lam511, ESC derived from 129 (E14, RG) and Pdgfra::GFP-F1 background (FL4, FL11) in 2i and 2i-LIF and embryonic samples from E1.5-5.5. (I) Time-lapse of single-cell ESC derivation on Fn-Lam511 in 2i-LIF at E4.5 using a destabilised Rex1-GFP reporter. (J) Model where individual preimplantation epiblast cells can be directly captured in an ESC state *in vitro*. Both states are naïve pluripotent, single-cell culture-permissive and closely related in their transcriptional program. Early ICM cells do not give rise to clonal ESC colonies directly, but can be rescued by either a 24h maturation step without FGF signalling inhibition or provision of Fn-Lam511, which mimics the embryonic extracellular matrix.